Joint Sensor Selection, Beamforming and Phase Control in Reconfigurable Intelligent Surface Aided IoT Fusion Networks

Yuyan Zhou, Yang Liu, *Member, IEEE*, Ming Li, *Senior Member, IEEE*, Qingqing Wu, and Hao Wang

***Abstract*—In this letter, we investigate the power minimization problem in an Internet of Things (IoT) sensor network assisted by reconfigurable intelligent surface (RIS). Different from the existing literature, we consider both transmit and non-transmit energy consumption, which leads to a joint sensor selection, beamforming design and RIS phase configuration problem. Based on the cutting-the-edge majorization minimization (MM) and penalty duality decomposition (PDD) frameworks, we develop two solutions which can achieve nearly identical performance as that of exhaustive search method. Extensive numerical results verify the great benefit in power saving via sensor selection and the deployment of RIS device.**

***Index Terms*—Reconfigurable intelligent surface (RIS), group-sparsity, IoT sensor network.**

I. Introduction

INTERNET of Things (IoT) technology will become a predominant driving force for the evolution of the next generation communication system and be widely deployed to realize connections of everything [1]. One classical IoT network deployment scenario with a fusion center (FC) is originally proposed in [2] and has been cast with great attention till nowadays due to the constantly emerging novel applications over it, e.g., [3]–[5]. As mentioned by [1], power consumption and energy efficiency will become a key performance indicator (KPI) for future IoT applications. For instance, [3] proposes interference aware power determination (IAPD) scheme and [4] adopts hybrid beamforming to reduce power consumption. The authors in [5] consider power minimization problem under a newly proposed two-timescale frame structure. However the above works [3]–[5] only focus on the pure transmission power. In fact, as pointed out by [6]–[7], the non-transmit energy expenditure, including the circuit power, heat dissipation, signal processing and so on, can take a large share of the total power consumption and should not be ignored. In this respect, it would be beneficial to put a portion of the sensors into "sleep" mode to save energy, which has never been considered in the previous study [2]–[5].

Manuscript received October 26, 2021; accepted November 14, 2021. Date of publication November 23, 2021; date of current version February 17, 2022. This work was supported by the Dalian University of Technology under Grant DUT20RC(3)029. The work of Ming Li was supported by the National Natural Science Foundation of China under Grant 61971088. The work of Qingqing Wu was supported in part by the FDCT under Grant 0119/2020/A3 and Grant 0108/2020/A, and in part by the GDST under Grant 2021A1515011900 and Grant 2020B1212030003. The work of Hao Wang was supported by in part by the National Natural Science Foundation of China under Grant 12001367, and in part by the Natural Science Foundation of Shanghai under Grant 21ZR1442800. The associate editor coordinating the review of this article and approving it for publication was M. Hasna. *(Corresponding author: Yang Liu.)*

Yuyan Zhou, Yang Liu, and Ming Li are with the School of Information and Communication Engineering, Dalian University of Technology, Dalian 116024, China (e-mail: zyy98@mail.dlut.edu.cn; yangliu_613@dlut.edu.cn; mli@dlut.edu.cn).

Qingqing Wu is with the Department of Electrical and Computer Engineering, University of Macau, Macau, China (e-mail: qingqingwu@um.edu.mo).

Hao Wang is with the School of Information Science and Technology, ShanghaiTech University, Shanghai 201210, China (e-mail: wanghao1@shanghaitech.edu.cn).

Digital Object Identifier 10.1109/LWC.2021.3130145

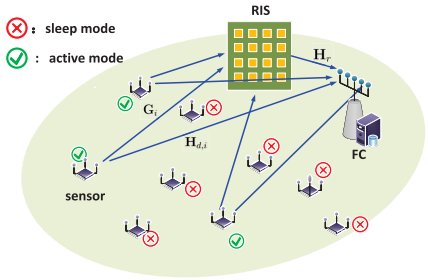

Fig. 1. A RIS-aided uplink IoT sensor network.

Besides considering wisely switching off sensor nodes, we also propose to exploit the promising reconfigurable intelligent surface (RIS) technology to further improve the power saving. Recently RIS has attracted great attention due to its remarkable advantage of low-cost and high energy efficiency. It is a planar surface comprising a great number of reflecting elements and can reflect the incident waves via dynamically adjusting their magnitudes and/or phase-shifts [8]. Research has proved the great potentials of RIS in power saving [9] and energy efficiency improvement [10]. Inspired by these works, here we introduce the RIS into the IoT network to further lower the power consumption.

Explicitly, our contributions are summarized as follows.

- Among the same line of research, e.g., [2]–[5], we are the first to consider non-transmit power consumption and the corresponding node selection problem which is highly challenging due to its combinatorial nature.
- We are the first to introduce RIS in the similar IoT network setting, which brings about the highly non-convex constant modulus constraints and makes the problem even more difficult.
- Two effective solutions are designed to attack the above difficult problem, which exhibit nearly identical performance with that of exhaustive search method. Besides, numerical results verify the great benefit in power saving via joint sensor selection and phase-shifting control.

II. Network Model and Problem Formulation

A. System Model

We consider a MIMO IoT wireless sensor network with L sensors as shown in Fig. 1. It is assumed that s is a source scalar with zero mean and unit variance. Each sensor independently obtains a noisy observation of the source and reports it to the fusion center [2].

The observation at the i-th sensor is modeled as $\mathbf{1}_{K_i}s+\mathbf{n}_i$, where K_i denotes the number of samples. $\mathbf{n}_i \in \mathbb{C}^{K_i\times 1}$ is the noise at i-th sensor independent from those of other sensors. For ease of analysis, we assume $\mathbf{n}_i \sim \mathcal{CN}(\mathbf{0}, \mathbf{\Sigma}_i)$.

It is assumed that the *i*-th sensor and the FC have N_i and M antennas, respectively. Each sensor employs a linear precoder $\mathbf{F}_i \in \mathbb{C}^{N_i \times K_i}$ to encode the observation before sending it to the FC. Via coordinating by a centric control node, the RIS can work collaboratively with sensors to intelligently enhance the propagation environment. The number of the reflecting units at the RIS is denoted by N. Let $\boldsymbol{\theta} = [\theta_1, \ldots, \theta_N]$ and $\boldsymbol{\phi} = [\mathrm{e}^{j\theta_1}, \ldots, \mathrm{e}^{j\theta_N}]^T$ denote phase-shifts and the corresponding reflecting coefficients, respectively. We also equivalently represent the RIS by a diagonal matrix $\boldsymbol{\Phi} = \mathrm{diag}(\boldsymbol{\phi})$. The channel between the *i*-th sensor to the FC, the *i*-th sensor to the RIS and the RIS to the FC are denoted by $\mathbf{H}_{d,i} \in \mathbb{C}^{M \times N_i}$, $\mathbf{G}_i \in \mathbb{C}^{N \times N_i}$ and $\mathbf{H}_r \in \mathbb{C}^{M \times N}$, respectively. The additive white gaussian noise at the FC is denoted by $\mathbf{n}_0 \in \mathbb{C}^{M \times 1}$. The received signal at the FC is given by:

$$\mathbf{r} = \sum_{i=1}^{L} (\mathbf{H}_{d,i} + \mathbf{H}_r \breve{\mathbf{G}}_i) \mathbf{F}_i \mathbf{1}_{K_i} s + \sum_{i=1}^{L} (\mathbf{H}_{d,i} + \mathbf{H}_r \boldsymbol{\Phi} \mathbf{G}_i) \mathbf{F}_i \mathbf{n}_i + \mathbf{n}_0. \quad (1)$$

In addition, by employing a linear receiving filter denoted by $\mathbf{w} \in \mathbb{C}^{\mathbf{M} \times 1}$, the SNR at the FC is defined in (2), shown at the bottom of the page.

B. Power Model

We here introduce a practical power consumption model. For an operating sensor, its energy expenditure comprises two parts, one is the transmission power P_i^{out}, which is given as $P_i^{\mathrm{out}} = \mathrm{Tr}(\mathbf{F}_i(\mathbf{1}_{K_i}\mathbf{1}_{K_i}^H + \boldsymbol{\Sigma}_i)\mathbf{F}_i^H)$, the other part P_i^{a} is the regular power consumption coming from signal processing, heat dissipation, circuitry power supply and so on. In fact, the power P_i^{a} required to maintain working properly can be much larger than the transmit power P_i^{out} [7]. Considering the fact that all sensors concurrently observe one common target signal, a portion of sensors can actually be put into sleep mode. A sleeping sensor consumes power at a much lower level of P_i^{s}. Let $\mathcal{L} = \{1, \ldots, L\}$ denote the set of all sensors, $\mathcal{A} \subseteq \mathcal{L}$ denote active sensor set, while $\mathcal{Z}$ denote the inactive set with $\mathcal{Z} \cup \mathcal{A} = \mathcal{L}$ and $\mathcal{Z} \cap \mathcal{A} = \emptyset$.

Therefore the overall power consumption model of a sensor is described as follows:

$$P_i^{\mathrm{sen}} = \begin{cases} P_i^{\mathrm{a}} + P_i^{\mathrm{out}}, & \text{if } P_i^{\mathrm{out}} > 0, \\ P_i^{\mathrm{s}}, & \text{if } P_i^{\mathrm{out}} = 0. \end{cases} \quad (3)$$

Each sensor has its own transmit power constraint:

$$\mathrm{Tr}(\mathbf{F}_i\Big(\mathbf{1}_{K_i}\mathbf{1}_{K_i}^H + \boldsymbol{\Sigma}_i\Big)\mathbf{F}_i^H) \le P_i, \forall i \in \mathcal{L}. \quad (4)$$

C. Problem Formulation

Based on the above elaboration, the network power consumption is given by

$$\begin{aligned} \tilde{p}(\mathcal{A}) &= \sum_{i \in \mathcal{A}} P_i^{\mathrm{out}} + \sum_{i \in \mathcal{A}} P_i^{\mathrm{a}} + \sum_{i \in \mathcal{Z}} P_i^{\mathrm{s}} \\ &= \sum_{i=1}^{L} P_i^{\mathrm{out}} + \sum_{i=1}^{L} \|\|\mathbf{F}_i\|_2^2\|_0 P_i^{\mathrm{d}} + \sum_{i=1}^{L} P_i^{\mathrm{s}}, \end{aligned} \quad (5)$$

where $P_i^{\mathrm{d}} = P_i^{\mathrm{a}} - P_i^{\mathrm{s}}$, and the last term in (5) is a constant. Hence minimizing the power consumption is equivalent to minimizing the redefined function:

$$P_{\mathrm{t}} = \sum_{i=1}^{L} \|\|\mathbf{F}_i\|_2^2\|_0 P_i^{\mathrm{d}} + \sum_{i=1}^{L} \mathrm{Tr}\Big(\mathbf{F}_i\Big(\mathbf{1}_{K_i}\mathbf{1}_{K_i}^H + \boldsymbol{\Sigma}_i\Big)\mathbf{F}_i^H\Big). \quad (6)$$

In this work, we assume channel status information (CSI) is available. With the SNR target γ, the problem of joint sensor selection, beamforming and RIS phase-shifts configuration towards power minimization is formulated as:

$$\begin{aligned} (\mathrm{P}\,1): \min_{\{\mathbf{F}_i\}, \boldsymbol{\Phi}, \mathbf{w}} \quad & P_{\mathrm{t}}, & (7a) \\ \text{s.t.} \quad & \mathsf{SNR}(\mathbf{w}, \{\mathbf{F}_i\}, \boldsymbol{\Phi}) \ge \gamma, & (7b) \\ & \mathrm{Tr}\Big(\mathbf{F}_i\Big(\mathbf{1}_{K_i}\mathbf{1}_{K_i}^H + \boldsymbol{\Sigma}_i\Big)\mathbf{F}_i^H\Big) \le P_i, \forall i \in \mathcal{L}, & (7c) \\ & |\boldsymbol{\Phi}_{n,n}| = 1, n = 1, \ldots, N. & (7d) \end{aligned}$$

The problem (P1) is challenging due to the simultaneous presence of ℓ_0-norm in the objective, the non-convex SNR requirements and the bunch of constant modulus constraints.

III. Proposed Algorithm

In this section, we will develop a group-sparsity inducing based solution which has three stages. In the first stage, we transform the original combinatorial problem into a more tractable one via inducing the group sparsity structure in the beamforming design. Then, in the second stage, we will rank the sensors to obtain a "turn-off" priority that fully exploits the sparsity structure of the previously obtained solution and then select the sensors based on the ranking. In the last stage, we can finally obtain the optimized beamformer and RIS phase-shifting under the known active sensor set. The details will be presented in the next subsections.

A. Stage I: Inducing Group-Sparsity Structure

In this subsection, we will develop an algorithm to induce group sparsity structure in the beamformer and adopt the alternative optimization methodology to optimize the variables $\{\mathbf{F}_i\}$, $\mathbf{w}$ and $\boldsymbol{\Phi}$ iteratively. For given $\boldsymbol{\Phi}$ and $\{\mathbf{F}_i\}$, $\mathbf{w}$ only exists in the SNR constraint, so the optimization problem can be reformulated as:

$$(\mathrm{P}\,2): \max_{\mathbf{w}} \ \frac{\mathbf{w}^H \mathbf{a}\mathbf{a}^H \mathbf{w}}{\mathbf{w}^H \mathbf{B} \mathbf{w}} \quad (8)$$

where $\mathbf{H}_{eq,i} = \mathbf{H}_{d,i} + \mathbf{H}_r \boldsymbol{\Phi} \mathbf{G}_i$, $\mathbf{a} = \sum_{i=1}^{L} \mathbf{H}_{eq,i} \mathbf{F}_i \mathbf{1}_{K_i}$, $\mathbf{B} = \sum_{i=1}^{L} \mathbf{H}_{eq,i} \mathbf{F}_i \boldsymbol{\Sigma}_i \mathbf{F}_i^H \mathbf{H}_{eq,i}^H + \boldsymbol{\Sigma}_0$. By Rayleigh-Ritz theorem, the optimal solution is given as:

$$\mathbf{w}^* = \mathbf{B}^{-1}\mathbf{a}. \quad (9)$$

We now proceed to optimize $\{\mathbf{F}_i\}_{i=1}^L$ when $\boldsymbol{\Phi}$ and $\mathbf{w}$ are given. First we introduce the notations $b \triangleq \mathrm{tr}\,(\mathbf{W}\boldsymbol{\Sigma}_0)$, $\mathbf{f}_i \triangleq \mathrm{vec}\,(\mathbf{F}_i)$, $\mathbf{f} \triangleq \{\mathbf{f}_i^T, \ldots, \mathbf{f}_L^T\}^T$, $\mathbf{E}_i \triangleq (\mathbf{1}_{K_i}\mathbf{1}_{K_i}^H + \boldsymbol{\Sigma}_i)^T \otimes \mathbf{I}_{N_i}$, $\mathbf{D}_i \triangleq \mathrm{diag}\{\mathbf{O}_{\sum_{j=1}^{i-1} K_j N_j}, \mathbf{E}_i, \mathbf{O}_{\sum_{j=i+1}^{L} K_j N_j}\}$, $\mathbf{c} \triangleq \{\mathbf{w}, \ldots, \mathbf{w}\}$, $\mathbf{R}_i \triangleq \boldsymbol{\Sigma}_i \otimes (\mathbf{H}_{eq,i}^H \mathbf{W} \mathbf{H}_{eq,i})$, $\mathbf{R} \triangleq \mathrm{diag}\{\mathbf{R}_1, \ldots, \mathbf{R}_L\}$, $\mathbf{G}_i \triangleq \mathrm{diag}\{\mathbf{O}_{\sum_{j=1}^{i-1} K_j N_j}, \mathbf{I}_{N_i K_i}, \mathbf{O}_{\sum_{j=i+1}^{L} K_j N_j}\}$, $\mathbf{Q}_i \triangleq \mathbf{1}_{K_i}^T \otimes \mathbf{H}_{eq,i}$ $\mathbf{Q} \triangleq \mathrm{diag}\{\mathbf{Q}_1, \ldots, \mathbf{Q}_L\}$. By the identity $\mathrm{Tr}\{\mathbf{ABCD}\} = \mathrm{diag}(\mathbf{D}^T)[\mathbf{C}^T \otimes \mathbf{A}]\mathrm{vec}(\mathbf{B})$, we rewrite the problem with

$$\mathsf{SNR}(\mathbf{w}, \{\mathbf{F}_i\}, \boldsymbol{\Phi}) = \frac{\sum_{i=1}^{L} \left|\mathbf{w}^H \left(\mathbf{H}_{d,i} + \mathbf{H}_r \boldsymbol{\Phi} \mathbf{G}_i\right) \mathbf{F}_i \mathbf{1}_{K_i}\right|^2}{\sum_{i=1}^{L} \mathbf{w}^H \left(\mathbf{H}_{d,i} + \mathbf{H}_r \boldsymbol{\Phi} \mathbf{G}_i\right) \mathbf{F}_i \boldsymbol{\Sigma}_i \mathbf{F}_i^H \left(\mathbf{H}_{d,i} + \mathbf{H}_r \boldsymbol{\Phi} \mathbf{G}_i\right)^H \mathbf{w} + \mathbf{w}^H \boldsymbol{\Sigma}_0 \mathbf{w}} \quad (2)$$

respect to $\{\mathbf{F}_i\}_{i=1}^L$ in the form as:

$$(\mathrm{P}\,3):\ \min_{\mathbf{f}}\ \sum_{i=1}^{L}\|\|\mathbf{f}^H\mathbf{G}_i\|_2^2\|_0 P_i^{\mathrm{d}}+\sum_{i=1}^{L}\mathbf{f}^H\mathbf{D}_i\mathbf{f}, \quad (10a)$$

$$\text{s.t. } \sqrt{\gamma}\sqrt{\|\mathbf{R}^{\frac{1}{2}}\mathbf{f}\|_2^2+b}\le \mathrm{Re}\{\mathbf{c}^H\mathbf{Q}\mathbf{f}\}, \quad (10b)$$

$$\mathrm{Im}\{\mathbf{c}^H\mathbf{Q}\mathbf{f}\}=0, \quad (10c)$$

$$\mathbf{f}^H\mathbf{D}_i\mathbf{f}\le P_i,\ \forall i\in L. \quad (10d)$$

The constraint (7b) is transformed to a second order cone (SOC) constraint, since it is not sensitive to the phase of $\mathbf{F}$, therefore we have (10c) established without losing optimality of the solution. However, the problem is still non-convex due to the ℓ_0-norm. Inspired by [7], we employ the re-weighted ℓ_1/ℓ_2-norm to approximate it. The objective function in (10a) is rewritten as:

$$\tilde{p}(\mathbf{f}|\alpha_i)=\sum_{i=1}^{L}\alpha_i\|\mathbf{f}_i\|_2^2P_i^{\mathrm{d}}+\sum_{i=1}^{L}\mathbf{f}^H\mathbf{D}_i\mathbf{f}. \quad (11)$$

Therefore this problem is reformulated as:

$$(\mathrm{P}\,4):\ \min_{\mathbf{f}}\ \tilde{p}(\mathbf{f}|\alpha_i), \quad (12a)$$

$$\text{s.t. } (10b),\ (10c),\ (10d), \quad (12b)$$

where α_i is a weighting coefficient given by:

$$\alpha_i^{t+1}=\frac{1}{\|\mathbf{f}_i^t\|_2^2+\tau},\ \forall i\in\mathcal{L}. \quad (13)$$

The solution $\mathbf{f}_i^t$ is obtained in the previous iteration and τ is a small positive constant to avoid ill-conditional behavior when $\mathbf{f}_i^t$ is close to zero [7]. The problem is convex and can be numerically solved via CVX. It can be seen from (13), when the beamformer has a low transmit power, the corresponding weight becomes large to force the transmit power to be further reduced in the next iteration. Furthermore, other methods such as the arctangent function [6] can also be applied, whose performance will be presented in Section IV.

Next, we focus on optimizing the phase shifts $\boldsymbol{\phi}$. The optimization problem is formulated as follows:

$$(\mathrm{P}\,5):\ \min_{\beta,\boldsymbol{\phi}}\ \beta, \quad (14a)$$

$$\text{s.t. } \gamma\mathbf{g}_2(\boldsymbol{\phi})-\mathbf{g}_1(\boldsymbol{\phi})\le\beta, \quad (14b)$$

$$|\boldsymbol{\phi}_n|=1,\forall n\in N, \quad (14c)$$

The parameters in (14b) are defined in (15), shown at the bottom of this page. Observing that the constraint (14b) is the difference of two convex functions, we employ majorization-minimization (MM) method [12]. Using the first order Taylor expansion at the point of $\boldsymbol{\phi}=\boldsymbol{\phi}^t$, we linearize $\mathbf{g}_1(\boldsymbol{\phi})$ to obtain an upper bound at the t-th iteration:

$$\tilde{\mathbf{g}_1}(\boldsymbol{\phi})\triangleq\mathbf{g}_1(\boldsymbol{\phi}^t)+2\,\mathrm{Re}\Big\{\Big[(\boldsymbol{\phi}^t)^H\mathbf{A}_1+\mathbf{d}_1^H\Big](\boldsymbol{\phi}-\boldsymbol{\phi}^t)\Big\}. \quad (16)$$

In the following, we will provide two alternative methods to address the non-convex unit modulus constraint (14c).

1) MM Method: Noting the fact that the constraint (14b) is indeed active when achieving optimality, therefore we can equivalently transform the problem (P5) into

$$(\mathrm{P}\,6):\ \min_{\boldsymbol{\phi}}\ \gamma\mathbf{g}_2(\boldsymbol{\phi})-\tilde{\mathbf{g}_1}(\boldsymbol{\phi}), \quad (17a)$$

$$\text{s.t. } |\boldsymbol{\phi}_n|=1,\forall n\in N. \quad (17b)$$

For any feasible $\boldsymbol{\phi}$ and $\boldsymbol{\phi}^t$, we have

$$\boldsymbol{\phi}^H\mathbf{A}_2\boldsymbol{\phi}\le\boldsymbol{\phi}^H\mathbf{X}_2\boldsymbol{\phi}-2\,\mathrm{Re}\Big\{\boldsymbol{\phi}^H(\mathbf{X}_2-\mathbf{A}_2)\boldsymbol{\phi}^t\Big\}+\big(\boldsymbol{\phi}^t\big)^H(\mathbf{X}_2-\mathbf{A}_2)\boldsymbol{\phi}^t, \quad (18)$$

where $\mathbf{X}_2=\lambda_{max}\mathbf{I}_N$ and λ_{max} is the maximum eigenvalue of $\mathbf{A}_2$. Noting the fact that $\boldsymbol{\phi}$ has constant modulus elements, $\boldsymbol{\phi}^H\mathbf{X}_2\boldsymbol{\phi}=N\lambda_{\max}$. Omitting the constants, the problem (P6) can be written as:

$$(\mathrm{P}\,7):\ \max_{\boldsymbol{\phi}}\ 2\mathrm{Re}\Big\{\boldsymbol{\phi}^H\mathbf{q}^t\Big\}, \quad (19a)$$

$$\text{s.t. } |\boldsymbol{\phi}_n|=1,\forall n\in N, \quad (19b)$$

where $\mathbf{q}^t=\gamma(\mathbf{X}_2-\mathbf{A}_2)\boldsymbol{\phi}^t-\gamma\mathbf{d}_2+\mathbf{A}_1\boldsymbol{\phi}^t+\mathbf{d}_1$. The optimal solution to the problem (P7) is given by:

$$\boldsymbol{\phi}^{t+1}=e^{j\arg(\mathbf{q}^t)}. \quad (20)$$

2) PDD Method: To decouple the constraints (14b) and (14c), we firstly introduce a copy $\boldsymbol{\psi}$ of $\boldsymbol{\phi}$. To tackle the equalty constraint $\boldsymbol{\phi}=\boldsymbol{\psi}$, following the PDD framework [11], we turn to optimizing the augmented Lagrangian (AL) function, which is defined as:

$$(\mathrm{P}\,8):\ \min_{\beta,\boldsymbol{\phi},\boldsymbol{\psi},\boldsymbol{\lambda}}\ \beta+\frac{1}{2\rho}\|\boldsymbol{\phi}-\boldsymbol{\psi}\|_2^2+\mathrm{Re}\Big\{\boldsymbol{\lambda}^H(\boldsymbol{\phi}-\boldsymbol{\psi})\Big\}, \quad (21a)$$

$$\text{s.t. } \gamma\mathbf{g}_2(\boldsymbol{\phi})-\tilde{\mathbf{g}_1}(\boldsymbol{\phi})\le\beta, \quad (21b)$$

$$|\boldsymbol{\phi}_n|\le 1,\forall n\in N, \quad (21c)$$

$$|\boldsymbol{\psi}_n|=1,\forall n\in N, \quad (21d)$$

with $\boldsymbol{\lambda}$ being the dual variable corresponding to the equality constraint $\boldsymbol{\phi}=\boldsymbol{\psi}$ and ρ being the penalty parameter [11].

The PDD method is a two-layer iteration, with its inner layer alternatively updating $\boldsymbol{\phi}$ and $\boldsymbol{\psi}$, its outer layer selectively updating $\boldsymbol{\lambda}$ or ρ. As for the inner layer, when $\boldsymbol{\psi}$ is fixed, the update of $(\boldsymbol{\phi},\beta)$ is performed as follows:

$$(\mathrm{P}\,9):\ \min_{\beta,\boldsymbol{\phi}}\ \beta+\frac{1}{2\rho}\|\boldsymbol{\phi}-\boldsymbol{\psi}\|_2^2+\mathrm{Re}\Big\{\boldsymbol{\lambda}^H(\boldsymbol{\phi}-\boldsymbol{\psi})\Big\}, \quad (22a)$$

$$\text{s.t. } \gamma\mathbf{g}_2(\boldsymbol{\phi})-\tilde{\mathbf{g}_1}(\boldsymbol{\phi})\le\beta, \quad (22b)$$

$$|\boldsymbol{\phi}_n|\le 1,\forall n\in N. \quad (22c)$$

We can see this problem is convex and can be solved via CVX. When $(\boldsymbol{\phi},\beta)$ are given, $\boldsymbol{\psi}$ is solved by the problem:

$$(\mathrm{P}\,10):\ \min_{\boldsymbol{\psi}}\ \frac{1}{2\rho}\|\boldsymbol{\phi}-\boldsymbol{\psi}\|_2^2+\mathrm{Re}\Big\{\boldsymbol{\lambda}^H(\boldsymbol{\phi}-\boldsymbol{\psi})\Big\}, \quad (23a)$$

$$\text{s.t. } |\boldsymbol{\psi}_n|=1,\forall n\in N. \quad (23b)$$

We notice that $\frac{1}{2\rho}\|\boldsymbol{\psi}\|_2^2=\frac{N}{2\rho}$ when $\boldsymbol{\psi}$ has unit modulus entries. Hence the problem is reduced to:

$$\mathbf{g}_1(\boldsymbol{\phi})\triangleq\boldsymbol{\phi}^H\mathbf{A}_1\boldsymbol{\phi}+2\mathrm{Re}\Big\{\boldsymbol{\phi}^H\mathbf{d}_1\Big\}+a_1,\mathbf{g}_2(\boldsymbol{\phi})\triangleq\boldsymbol{\phi}^H\mathbf{A}_2\boldsymbol{\phi}+2\mathrm{Re}\Big\{\boldsymbol{\phi}^H\mathbf{d}_2\Big\}+a_2,\boldsymbol{\Lambda}_1\triangleq\sum_{i=1}^{L}\Big(\mathbf{w}^H\mathbf{H}_r\mathrm{diag}\big(\mathbf{G}_i\mathbf{F}_i\mathbf{1}_{K_i}\big)\Big)^H$$

$$\mathbf{A}_1\triangleq\boldsymbol{\Lambda}_1\boldsymbol{\Lambda}_1^H,\boldsymbol{\Lambda}_{2_i}\triangleq\mathbf{G}_i^H\mathrm{diag}\Big(\mathbf{H}_r^H\mathbf{w}\Big),a\triangleq\sum_{i=1}^{L}\mathbf{w}^H\mathbf{H}_{d,i}\mathbf{F}_i\mathbf{1}_{K_i},\mathbf{A}_2\triangleq\sum_{i=1}^{L}\Big(\boldsymbol{\Lambda}_{2_i}^H\mathbf{F}_i\boldsymbol{\Sigma}_i\mathbf{F}_i^H\boldsymbol{\Lambda}_{2_i}\Big)^*,\mathbf{d}_1\triangleq\boldsymbol{\Lambda}_1 a$$

$$\mathbf{d}_2\triangleq\sum_{i=1}^{L}\Big(\boldsymbol{\Lambda}_{2_i}^H\mathbf{F}_i\boldsymbol{\Sigma}_i\mathbf{F}_i^H\mathbf{H}_{d,i}^H\mathbf{w}\Big)^*,a_2\triangleq\sum_{i=1}^{L}\mathbf{w}^H\mathbf{H}_{d,i}\mathbf{F}_i\boldsymbol{\Sigma}_i\mathbf{F}_i^H\mathbf{H}_{d,i}^H\mathbf{w}+\mathbf{w}^H\boldsymbol{\Sigma}_0\mathbf{w},a_1\triangleq a^2 \quad (15)$$

Algorithm 1 Sensor Selection & Beamforming

1: Find feasible $\boldsymbol{w}^{(0)}$, $\boldsymbol{\Phi}^{(0)}$, $\{\mathbf{F}_i\}$, set $n=0$;
2: **repeat**
3: Update $\boldsymbol{w}^{(n+1)}$ by (9);
4: Update $\mathbf{F}^{(n+1)}$ by solving problem (P4);
5: Update $\Phi^{(n+1)}$ by solving problem (P6) or problem (P8);
6: **until** $\mathbf{F}$ obtain the group sparsity structure;
7: Obtain the solution of $\{\mathbf{F}_i\}$, calculate ordering criterion (27) and sort them in the ascending order $\delta_{\pi_1} \leq \delta_{\pi_2} \leq \cdots \leq \delta_{\pi_{\mathrm{L}}}$;
8: Initialize $J_{\mathrm{low}}=1$, $J_{\mathrm{up}}=L$;
9: **repeat**
10: Set $J \leftarrow [\frac{J_{\mathrm{low}}+J_{\mathrm{up}}}{2}]$;
11: Solve the problem $(\mathrm{P}\,11_{\mathcal{A}(J)})$: if it is feasible, set $J_{\mathrm{low}}=J$; otherwise, set $J_{\mathrm{up}}=J$;
12: **until** $J_{\mathrm{up}}-J_{\mathrm{low}}=1$, obtain $J_{\max}=J_{\mathrm{low}}$ and obtain the optimal active sensor set $\mathcal{A}^\star$ with $\mathcal{A}^\star \cup \mathcal{J}=\mathcal{L}$ and $\mathcal{J}=\{\pi_1,\pi_2,\cdots,\pi_{J_{\max}}\}$;
13: Solve the problem (P1) with the known active sensor set, and obtain the corresponding transmit beamformers and phase-shift at the RIS;

$$(\mathrm{P}\,10)'\colon \max_{\|\boldsymbol{\psi}\|=\mathbf{1}_N} \ \mathrm{Re}\Big\{(\boldsymbol{\phi}+\rho\boldsymbol{\lambda})^H\boldsymbol{\psi}\Big\}, \tag{24}$$

the optimal $\boldsymbol{\psi}$ is achieved when its elements are aligned with the phase of the complex vector $(\rho^{-1}\boldsymbol{\phi}+\boldsymbol{\lambda})$, thus

$$\boldsymbol{\psi}^\star = \exp(j\cdot\angle(\boldsymbol{\phi}+\rho\boldsymbol{\lambda})). \tag{25}$$

The inner layer alternatively updates $(\boldsymbol{\phi},\beta)$ and $\boldsymbol{\psi}$ until convergence is reached. For the outer layer update of the PDD procedure, two cases will occur. If the equality $\boldsymbol{\psi}=\boldsymbol{\phi}$ nearly holds, the Lagrangian multiplier will be updated as:

$$\boldsymbol{\lambda} = \boldsymbol{\lambda} + \rho^{-1}(\boldsymbol{\phi}-\boldsymbol{\psi}). \tag{26}$$

Otherwise, the penalty parameter ρ will be decreased to force the equality constraint $\boldsymbol{\phi}=\boldsymbol{\psi}$ to be approached.

B. Stage II: Sensor Selection

In this section, we will propose a sensor selection method based on the group sparsity solution.

1) Sensor Ordering: To simplify the sensor selection procedure, we first assign a switch-off priority to every sensor via exploiting the group sparsity structure of the previously obtained solution. Here we propose to use the beamforming energy as the priority metric, i.e.,

$$\delta_i = \|\mathbf{F}_i\|_F,\ \forall i \in \mathcal{L}. \tag{27}$$

Based on the metric in (27) we obtain a ranking $\delta_{\pi_1} \leq \delta_{\pi_2} \leq \cdots \leq \delta_{\pi_{\mathrm{L}}}$, which implies that the rank $\delta_{\pi_{\mathrm{i}}}$ with a lower index *i* has a high priority to be switched off.

2) Bisection Search Procedure: For sensor node selection, we always switch off the nodes associated with the highest turn-off priorities first. That means we need to identify the largest integer $J_{\max}$ such that sensors indexed by $\{\pi_1,\pi_2,\ldots,\pi_{J_{\max}}\}$ are switched off while the others are activated. For each specific *J*, define the active sensor set $\mathcal{A}(J) \triangleq \{\pi_{J+1},\ldots,\pi_L\}$ with $\mathcal{A}(J)\cup\mathcal{Z}(J)=\mathcal{L}$. We need to determine its feasibility by solving the problem $(\mathrm{P}\,11_{\mathcal{A}(J)})$:

$$\begin{aligned}
\Big(\mathrm{P}\,11_{\mathcal{A}(J)}\Big)\colon\ & \mathrm{find}\{\mathbf{F}_i\},\boldsymbol{\Phi},\mathbf{w}, && \text{(28a)}\\
& \text{s.t. } (7b),\ (7d), && \text{(28b)}\\
& \mathrm{Tr}\Big(\mathbf{F}_i\Big(\mathbf{1}_{K_i}\mathbf{1}_{K_i}^H+\boldsymbol{\Sigma}_i\Big)\mathbf{F}_i^H\Big) \leq P_i, \forall\, i\in\mathcal{A}(J), && \text{(28c)}\\
& \mathbf{F}_i=\mathbf{0},\ \text{if}\ \ i\in\mathcal{Z}(J). && \text{(28d)}
\end{aligned}$$

According to the feasibility of $(\mathrm{P}\,11_{\mathcal{A}(J)})$, we need to further determine the number of activated sensors until the maximal $J_{\max}$ is found. The whole search procedure can be done by a bisection search as described by line 8 to 12 in Algorithm 1.

C. Stage III: Transmit Beamforming and IRS Configuration

After identifying $\mathcal{A}^\star$ and $\mathcal{Z}^\star$, the problem (P1) can be easily solved following similar arguments as before. As for the initial point, we can solve the problem $(\mathrm{P}\,11_{\mathcal{A}(J)})$ with $\mathcal{A}(J)=\mathcal{L}$. Details are omitted due to space limit. As verified by numerical results, our proposed joint sensor selection and beamforming algorithm can perform nearly as well as the exhaustive search method. The whole algorithm is presented as Algorithm 1.

D. Complexity Analysis

Our proposed selection scheme is of $\mathcal{O}(\log(L))$ complexity. We assume that each sensor i has the same number of the antennas N_i and the samples K_i. The computational complexity of the proposed MM-based solution is $\mathcal{O}(\,M^2+C_1\,L^{1.5}\,(\,N_iK_i\,)^3\,+\,N^3\,)$. For the proposed PDD-based solution, the complexity is $\mathcal{O}(\,M^2+C_1\,L^{1.5}\,(\,N_iK_i\,)^3\,+\,\sqrt{3}C_3C_2N^3\,)$, where C_1, C_2 and C_3 represent the iteration number to solve the problem (P4), (P9) and (P8), respectively. The typical values of them according to the simulation results are 30, 60 and 30, respectively.

IV. Simulation Results

In this section, numerical results are presented to verify our proposed algorithms. The experiment system comprises one FC which uses $M=4$ antennas and one RIS device with $N=40$ reflecting elements. The network comprises $L=15$ sensors and each is equipped with $N_i=2$ antennas. The sampling number $K_i=4$. The distance between the FC and the RIS is 15 meters (m) and it is assumed that a line-of-sight (LoS) propagation path between them exists. The 15 sensors are located in a row parallel to the RIS-FC line which is 2m apart and with a 0.5m spacing interval between the adjacent peers. Signals emitting from the sensors to both the FC and the RIS experience 10dB penetration loss, independent Rayleigh fading and a pathloss exponent of 3. The noise at the *i*-th sensor and the FC both have the power of $1\times10^{-7}\,\mathrm{mW}$. We set the transmission power limit of each sensor as 2mW and $P_i^{\mathrm{d}}=4\,\mathrm{mW}$. Besides, it is assumed that the antenna gain of both the FC and the sensors is 0dBi and that of each reflecting element at the RIS is 5dBi.

Fig. 2 illustrates the convergence behavior of our proposed algorithms. The left one demonstrates the PDD algorithm's performance for solving (P8). The number of reflecting elements *N* varies from 20 to 80. The figure plots the difference between $\boldsymbol{\phi}$ and $\boldsymbol{\psi}$ along with the progress of PDD iterations. As shown by the results, the PDD algorithm generally converges within 30 iterations. In the right half of Fig. 2, we present the convergence property of the PDD-based and MM-based solutions to obtain the group sparsity beamforming in Stage I. The horizon axis represents the outer layer iteration index of the block coordinate decent (BCD) procedure. In the experiment, the two peer solutions start from identical initial points and exhibit almost identical performance.

In Fig. 3, for comparison, we present the performance associated with various sensor selection schemes that are elaborated in order: 1) coordinated beamforming algorithm (CB): all the sensors are activated. 2) exhaustive search: we enumerate all possible sensor selection patterns, perform beamforming optimization when feasible, and finally choose the selection pattern corresponding to the minimal total power. 3) arctangent function: we adopt the arctangent function in [6] as an alternative approximation method in addition to the ℓ_1/ℓ_2-norm and apply the MM method to updating the RIS phase-shifts. 4) random RIS: we do not optimize the phase-shifts of the

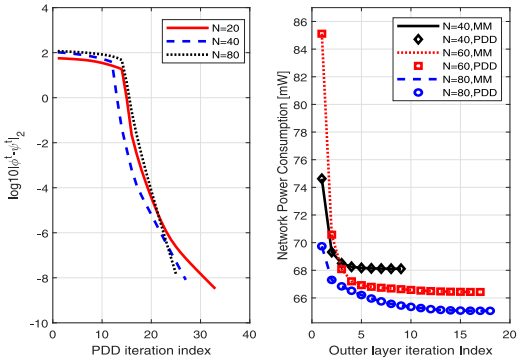

Fig. 2. Convergence of proposed algorithms.

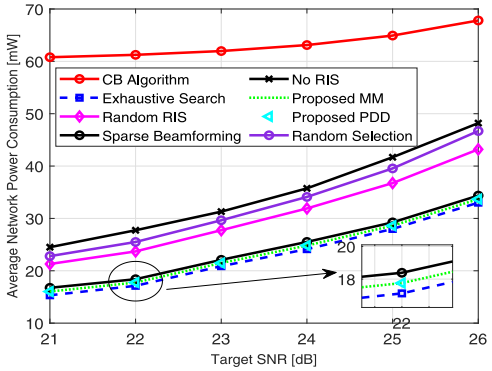

Fig. 3. Average power consumption versus target SNR.

TABLE I
PERFORMANCE OF VARIOUS SENSOR SELECTION SCHEMES

Target SNR [dB]	21	22	23	24	25	26
Exhaustive Search	2.73	3.15	3.80	4.15	5.07	5.83
Arctangent Fun.	3.05	3.42	3.97	4.54	5.29	5.95
Random Selection	4.36	4.83	5.33	6.18	6.93	8.54
Random RIS	3.84	4.16	4.90	5.58	6.37	7.47
No RIS	4.83	5.20	5.87	6.54	7.44	8.63
PDD-based So.	2.94	3.33	3.88	4.44	5.20	5.88
MM-based So.	2.94	3.33	3.88	4.44	5.20	5.88

RIS. 5) no RIS: only direct communication channel exists without employing the RIS. 6) random selection: we select the activated sensors without ranking randomly. 7) proposed MM-based solution: we optimize the phase-shifts with the MM method. 8) proposed PDD-based solution: we optimize the phase-shifts using the PDD method. In the experiment, we randomly generate 30 channel realizations and execute different sensor selection schemes for each specific channel realization. Fig. 3 demonstrates the average network power consumption with different target SNRs. This figure shows that our proposed PDD-based and MM-based solutions can achieve almost identically optimal performance which is obtained via the exhaustive search. Compared to the random RIS scheme, the advantage in power saving by the RIS optimization schemes demonstrates the benefit coming from the passive beamforming. This figure also reflects that our proposed schemes can reduce power consumption by up to 75% compared to the CB algorithm when under the low SNR constraint. As shown in the figure, both of the ℓ_1/ℓ_2-norm and arctangent function approximation methods can achieve nearly identical results.

In Table I, we present the number of activated sensors via different schemes. In this experiment, we randomly generate 30 channel realizations and report the average results again.

TABLE II
THE IMPACT OF RIS REFLECTING ELEMENTS

Target SNR [dB]	21	22	23	24	25	26
N=20	3.38	3.69	4.38	4.88	5.75	6.75
N=40	2.94	3.33	3.88	4.44	5.20	5.88
N=60	2.42	2.98	3.16	3.95	4.42	5.08
N=80	2.00	2.13	2.81	3.00	3.69	4.07

By the result, the PDD-based solution and the MM-based solution utilizing arctangent approximation yield almost identical number of activated sensors as that obtained by the exhaustive search scheme. Meanwhile, the random RIS scheme results in larger number of activated sensors, which demonstrates the beamforming gain from the phase-shift configuration.

Table II shows the impact of the number of the reflecting elements of the RIS on power consumption. With the number of reflecting elements increasing, the number of the activated sensors is reduced and total network power consumption is decreased accordingly. With a larger N, the RIS introduces larger flexibility in system design, which leads to higher beamforming gain and brings more benefit for power saving.

V. CONCLUSION

In this letter, we consider power minimization including both transmit and non-transmit energy in an RIS-assisted IoT sensor network. By jointly selecting the active sensors, optimizing coordinated beamforming and carefully tuning the phase-shifts at the RIS, the overall network power consumption can be significantly reduced. Extensive simulations verify the effectiveness of our proposed algorithms.

REFERENCES

[1] W. Jiang, B. Han, M. A. Habibi, and H. D. Schotten, "The road towards 6G: A comprehensive survey," *IEEE Open J. Commun. Soc.*, vol. 2, pp. 334–366, 2021.
[2] J.-J. Xiao, S. Cui, Z.-Q. Luo, and A. J. Goldsmith, "Linear coherent decentralized estimation," *IEEE Trans. Signal Process.*, vol. 56, no. 2, pp. 757–770, Feb. 2008.
[3] B. M. Lee, "Cell-free massive MIMO for massive low power Internet of Things networks," *IEEE Internet Things J.*, early access, Sep. 13, 2021, doi: 10.1109/JIOT.2021.3112195.
[4] H. Liu, S. Wang, X. Zhao, S. Gong, N. Zhao, and T. Q. S. Quek, "Analog–digital hybrid transceiver optimization for data aggregation in IoT networks," *IEEE Internet Things J.*, vol. 7, no. 11, pp. 11262–11275, Nov. 2020.
[5] X. Zhai, X. Chen, and Y. Cai, "Power minimization for massive MIMO over-the-air computation with two-timescale hybrid beamforming," *IEEE Wirelss Commun. Lett.*, vol. 10, no. 4, pp. 873–877, Apr. 2021.
[6] M. Tao, E. Chen, H. Zhou, and W. Yu, "Content-centric sparse multicast beamforming for cache-enabled cloud RAN," *IEEE Trans. Wireless Commun.*, vol. 15, no. 9, pp. 6118–6131, Sep. 2016.
[7] X. Peng, Y. Shi, J. Zhang, and K. B. Letaief, "Layered group sparse beamforming for cache-enabled green wireless networks," *IEEE Trans. Commun.*, vol. 65, no. 12, pp. 5889–5603, Dec. 2017.
[8] Q. Wu, S. Zhang, B. Zheng, C. You, and R. Zhang, "Intelligent reflecting surface-aided wireless communications: A tutorial," *IEEE Trans. Commun.*, vol. 69, no. 5, pp. 3313–3351, May 2021.
[9] Q. Wu and R. Zhang, "Intelligent reflecting surface enhanced wireless network via joint active and passive beamforming," *IEEE Trans. Wireless Commun.*, vol. 18, no. 11, pp. 5394–5409, Nov. 2019.
[10] C. Huang, A. Zappone, G. C. Alexandropoulos, M. Debbah, and C. Yuen, "Reconfigurable intelligent surfaces for energy efficiency in wireless communication," *IEEE Trans. Wireless Commun.*, vol. 18, no. 8, pp. 4157–4170, Aug. 2019.
[11] Q. Shi and M. Hong, "Penalty dual decomposition method for nonsmooth nonconvex optimization—Part I: Algorithms and convergence analysis," *IEEE Trans. Signal Process.*, vol. 68, pp. 4108–4122, Jun. 2020, doi: 10.1109/TSP.2020.3001906.
[12] Y. Sun, P. Babu, and D. P. Palomar, "Majorization-minimization algorithms in signal processing, communications, and machine learning," *IEEE Trans. Signal Process.*, vol. 65, no. 3, pp. 794–816, Feb. 2017.